Lithium ion battery recycling using high-intensity ultrasonication

Chunhong Lei, [a,b] Iain Aldous, [c] Jennifer M. Hartley, [a,b] Dana L. Thompson, [a,b] Sean Scott, [a,b] Rowan Hanson,[c] Paul A. Anderson, [b,d] Emma Kendrick,[b,e] Rob Sommerville,[b,e] Karl S. Ryder, [a,b] Andrew P. Abbott*[a,b]

[a] *School of Chemistry, University of Leicester, Leicester, UK, LE1 7RH*

[b] *The Faraday Institution, Quad One, Harwell Science and Innovation Campus, Didcot, UK*

[c] *College of Science & Engineering, Swansea University, UK, SA1 8EN*

[d] *School of Chemistry, University of Birmingham, Birmingham, UK, B15 2TT*

[e] *School of Metallurgy and Materials, University of Birmingham, Birmingham, UK, B15 2TT*

* Contact email: apa1@le.ac.uk

Supplementary Information
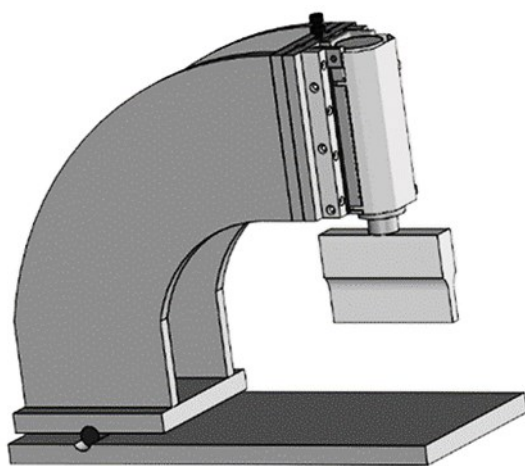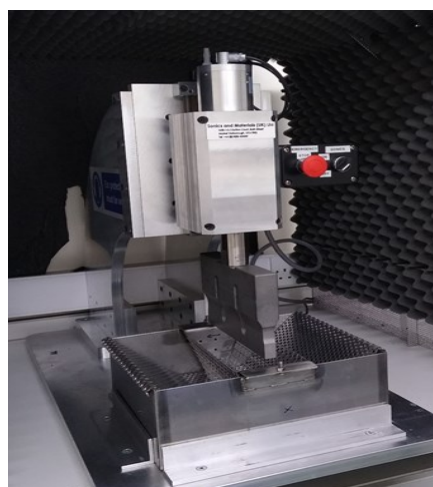
Figure S1: a) Ultrasonic system for electrode delamination, consisting of a converter, booster and sonotrode, all connected as a stack, and mounted on a frame. b) Photograph of apparatus.

The apparatus shown in Figure S1 was used for continuous flow delamination. The electrodes were fed in manually for the purposes of the experiments described in the text although an automated feed is currently being built. The electrodes pass through a basket which maintains an optimal distance from the sonotrode and clean foils are removed at the other side of the sonotrode.

Ultrasonication delamination theory

The acoustic wave pressure amplitude just outside of the oscillating front surface of the sonotrode can be calculated using **equation S1**:[1]

$$P_s = (2I\rho_0 c_0)^{1/2}$$

Eq. S1

where P_s is the acoustic wave pressure amplitude (Pa), I is the power intensity or surface power density (W/m^2) of the sonotrode, ρ_0 is the liquid density (kg/m^3), and c_0 is the acoustic velocity in the liquid (m/s). A high power intensity therefore results in large acoustic pressure. The threshold of the acoustic pressure amplitude for a cavitation initiation in distilled water is 0.06~0.1 MPa,[2] corresponding to a power intensity of 1.2~3.3 W/cm^2. The dimensionless ultrasonic cavitation number C_u is described by **equation S2**:

$$C_u = \frac{P - P_v}{P_s}$$

Eq. S2

where P is the local pressure amplitude, P_v is the vapour pressure of the liquid, and P_s is again the pressure amplitude near the sonotrode. A greater number of cavitation bubbles corresponds to a higher local acoustic pressure. These cavitation bubbles can interfere with the propagation of the pressure wave, which in turn affects the distribution of these bubbles. The interaction between the cavitation and the pressure wave dominates the power intensity distribution in high power sonicating systems. For example, when increasing power intensity to 8 W/cm^2, a cone-like bubble structure is formed underneath the sonotrode, and increasing the power density further to 80 W/cm^2 results in a chaotic jet of cavitation turbulence.[3, 4] The pressure wave originating from the sonotrode front surface will be distorted and dissipated by the cavitation cluster, resulting in a rapid drop of intensity with increasing distance from the front surface of the sonotrode,[5, 6] decreasing delamination strength. The attenuation of the cavitation cluster to the wave amplitude is reported to be around one tenth of that without the shielding of the cluster.[7] On the other hand, the cavitation cluster is beneficial in destroying the solid material it encounters, as it deforms or dents a solid surface in an average diameter of 10 μm through micro-jet and shock waves when collapsed.[8]

The sizes and lifetimes of these bubbles are related to the physical properties of the solution, including surface tension, density, viscosity, compressibility, and vapour pressure. For example, in ethanol, which has lower surface tension than water, the bubbles are larger and have longer lifetimes before their collapse. Larger bubbles tend to collapse more violently than the smaller ones, resulting in stronger erosion behaviour at the liquid-solid interface. The high

density cavitation absorbs and scatters the sound waves, thereby substantially weakening the acoustic intensity away from the conical structure zone. In glycerine, the cavitation intensity is larger near the sonotrode, but is greatly attenuated over distance due to the high solvent viscosity.[9]

After exposure to ultrasonic cavitation, denting and wrinkling was observed on a 30 μm thick aluminium foil (**Figure S2**). These pits and dents have rough bottoms, indicating that they are caused by cluster cavitation or consecutive cavitation.[8, 10] Optical microscope images of one of these pits is shown in **Figure S3**. The irregular bulge was caused by the pressure wave, which vibrates and deforms the foil across large areas in the direction perpendicular to the foil surface. The cavitation density and pressure wave intensity decrease rapidly with the distance from the sonotrode.

a)   b)   c)
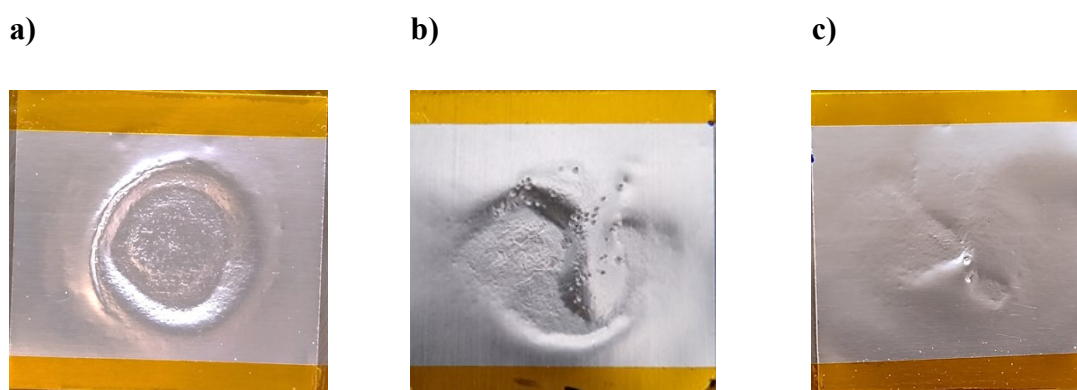
Figure S2: Images showing the effect of ultrasound on 30 μm thick aluminium foil in deionized water at: a) 2.5 mm, b) 5 mm, and c) 10 mm away from sonotrode. Sample size of 3 cm x 3 cm. The sonotrode was 20 mm in diameter, with 120 W/cm^2 power intensity applied for 3 seconds.

Therefore, in order to delaminate an electrode sheet from an electric vehicle effectively, the electrode sheet should be passed closely to the sonotrode tip, where pressure waves are strong and cavitation density is high. The pressure waves vibrate the electrode sheet and generate cavitation in the interface between the coating and the current collector, where imperfect sites locate, such as crack and pore, as cavitation tends to develop from a defect site. The combined action of pressure waves and cavitation can effectively delaminate the electrode coatings.
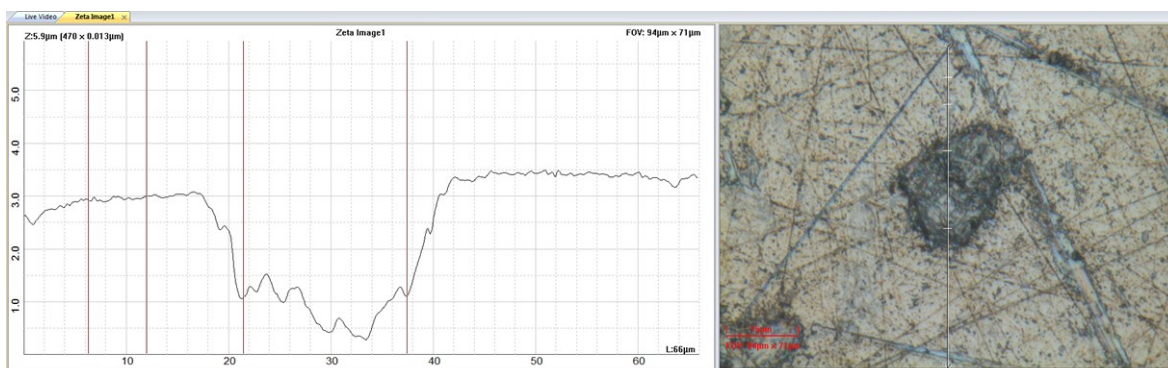
Figure S3: Optical microscope images (magnification amount) of the 'pitting' observed in the current collectors during ultrasonic delamination.
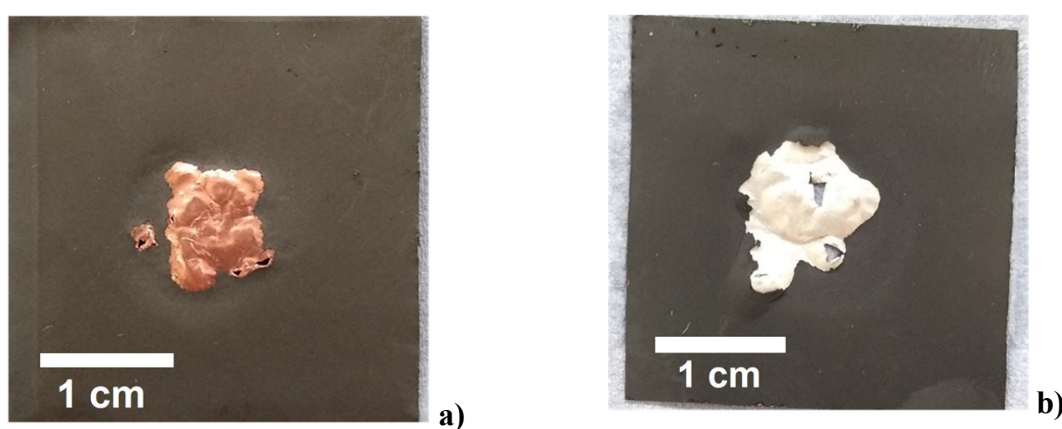
Figure S4: Images showing the effect of ultrasound on the back side of: a) lithium ion battery anode sheet, and b) lithium ion battery cathode sheet. The anode was delaminated in a solution of 0.05 M citric acid; the cathode was delaminated in a solution of 0.1 M NaOH. The sonotrode was 20 mm in diameter, with 120 W/cm² power intensity applied for 3 seconds, at 2.5 mm away from the sonotrode. Sample size was 3 cm x 3 cm.

Delamination of the electrode coatings results in minimal morphological changes to both the cathode and anode as observed in the scanning electron microscopy images in **Figure S5**. The differences in the images largely stem from changes to the macrostructure of the material as it is converted from an electrode coating to a powder, in the case of the cathode. In the case of the anode material, small particles that were formerly distributed across the graphite are absent after ultrasonication. These particles are most likely the carbon black conductive additive and could account for the particles below 3 μm in size which remain in the delaminating solution following the ultrasonication procedure.
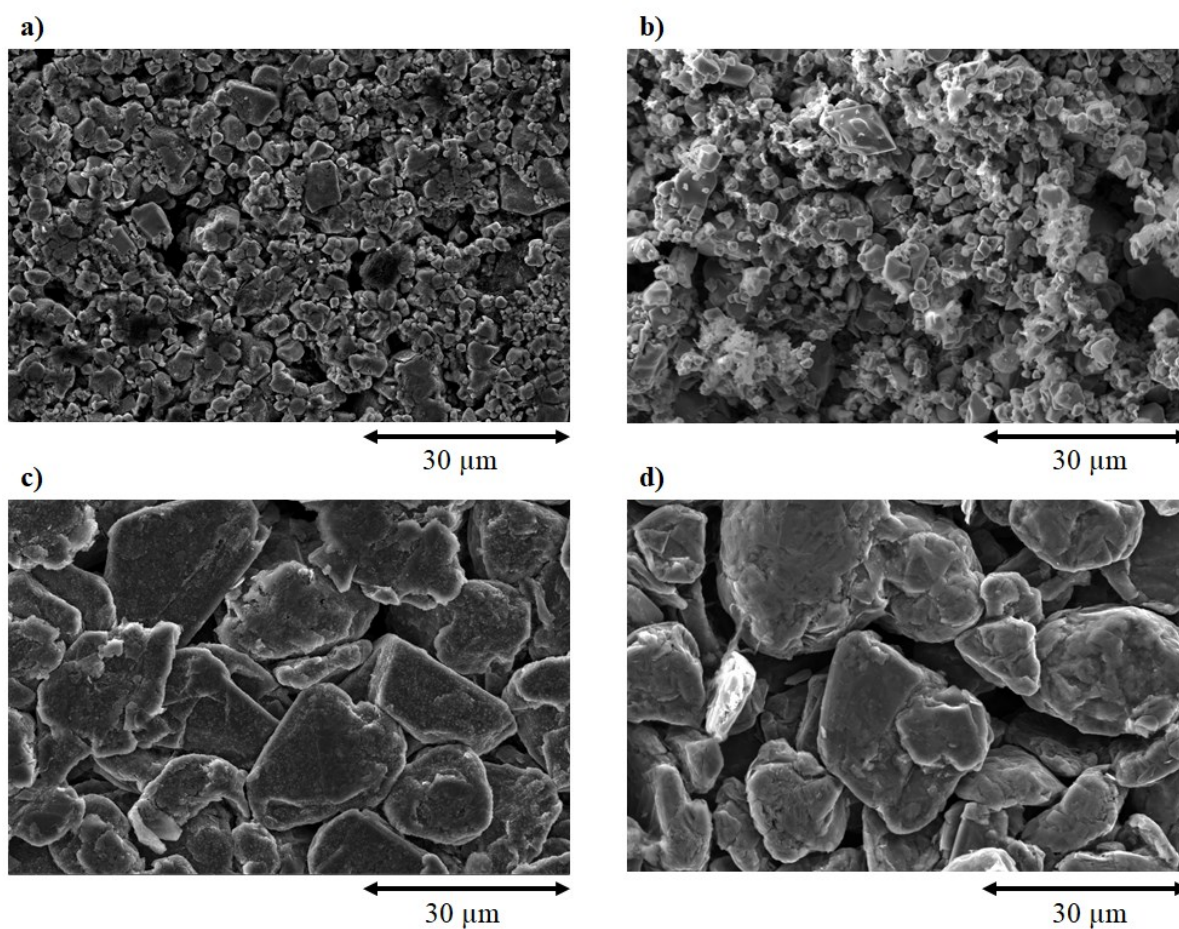
Figure S5: Scanning electron microscopy images showing the morphological changes to the electrode active material upon ultrasonic delamination. All images were taken at a 5000x magnification and 10 kV excitation energy. a) cathode material pre-delamination, b) delaminated cathode active material, c) anode material pre-delamination and d) delaminated anode material.

References

1. R. W. Time and A. H. Rabenjafimanantsoa, *Annual Transactions of The Nordic Rheology Society*, 2011, **19**, 1-12.

2. G. I. Eskin and D. G. Eskin, *Ultrasonic Treatment of Light Alloy Melts, Second Edition*, Taylor & Francis, 2014.

3. A. Moussatov, C. Granger and B. Dubus, *Ultrasonics Sonochemistry*, 2003, **10**, 191-195.

4. X. Ma, B. Huang, G. Wang and M. Zhang, *Ultrason Sonochem*, 2017, **34**, 164-172.

5. B. Dubus, C. Vanhille, C. Campos-Pozuelo and C. Granger, *Ultrason Sonochem*, 2010, **17**, 810-818.

6. L. Bai, J. Deng, C. Li, D. Xu and W. Xu, *Ultrason Sonochem*, 2014, **21**, 121-128.

7. I. Tzanakis, G. S. B. Lebon, D. G. Eskin and K. Pericleous, *Materials & Design*, 2016, **90**, 979-983.

8. I. Tzanakis, D. G. Eskin, A. Georgoulas and D. K. Fytanidis, *Ultrason Sonochem*, 2014, **21**, 866-878.

9. I. Tzanakis, G. S. Lebon, D. G. Eskin and K. A. Pericleous, *Ultrason Sonochem*, 2017, **34**, 651-662.

10. M. Dular, O. C. Delgosha and M. Petkovsek, *Ultrason Sonochem*, 2013, **20**, 1113-1120.